

# Structural Properties of $(\text{SnO}_2)_{1-x}(\text{ZnO})_x$ Thin Films Deposited By Spray Pyrolysis Technique

Nahida Bukheet Hasan, Zahra'a Adel Jawad

Department of Physics, College of Science, University of Babylon, Iraq

**Abstract**— Nano structure of mixed  $(\text{SnO}_2)_{1-x}(\text{ZnO})_x$  thin films were prepared by spray pyrolysis technique at a substrate temperature of  $400^\circ\text{C}$ . The films deposited were 190 nm thickness. The XRD analysis for its structural characteristic has been performed. The average grain size was found to be between 21.27 and 15.80 nm. AFM Atomic Force microscope gives good information about the surface topography of the film. It is understood that the crystallinity of  $\text{SnO}_2$  increases with increasing ZnO Vol.%.  
**Keywords**— Spray pyrolysis, tin oxide, zinc oxide, structural properties, and thin films.

## I. INTRODUCTION

Transparent conducting oxide (TCO) of thin films such as  $\text{ZnO}$ ,  $\text{SnO}_2$ ,  $\text{PbO}$ ,  $\text{CdO}$ ,  $\text{In}_2\text{O}_3$  and  $\text{MoO}_3$  have been studied in detail by many researchers [Cruz *et al.*, 2005; Ferro *et al.*, 2000]. These TCOs find extensive applications in thin film transistors, solar cells, phototransistors, optical storage devices, gas sensors, photo-thermal and photovoltaic conversions [Kumaravelet *et al.*, 2007]. Varieties of methods like dc reactive sputtering [Subramanyam *et al.*, 2001], chemical bath deposition [Ocampo *et al.*, 1994], activated reactive evaporation [K.T. Ramakrishna Reddy *et al.*, 1998], solution growth [Verky and Fort, 1994], thermal oxidation [Ferrer, 1993], sol-gel [Galicia, 2000], and spray pyrolysis have been reported in the preparation of  $\text{SnO}_2$  and  $\text{ZnO}$  thin films. The electro optical properties of  $\text{ZnO}$  make this material very convenient as a solar cell material [Ferro *et al.*, 2000]. Reportedly  $\text{SnO}_2$  exists in tetragonal ( $\alpha$ -phase) structures at low and high temperatures respectively. The difficulty of preparing exclusively single phase  $\text{SnO}_2$  was pointed out earlier. The  $\text{SnO}_2$  was obtained earlier by pulsed laser ablation [Baleva *et al.*, 1994] and spray pyrolysis [Thangarajuet *et al.*, 2000]. The  $\text{SnO}_2$  was transformed to the meta-stable  $\text{SnO}_2$  when heat treated beyond  $489^\circ\text{C}$  [Kirkbiret *et al.*, 1992]. In attempts to improvise the properties of  $\text{SnO}_2$ , it is being tried out to mix with other oxides. Recently, Hosono *et al.*, [Trinquier and R. Hoffman, 1984] reported amorphous semiconductor  $(\text{SnO}_2)_{1-x}(\text{ZnO})_x$  thin films with a novel information about the carrier generation through the formation of oxygen vacancies. In the present work, we bring out a structural investigation on mixed  $(\text{SnO}_2)_{1-x}(\text{ZnO})_x$  thin films with

$0 \leq x \leq 1$  prepared by spray pyrolytic decomposition of aqueous solutions of tin and zinc acetates at  $400^\circ\text{C}$ .

## II. EXPERIMENTAL WORK

### 2.1. Solutions Preparation:

The  $(\text{SnO}_2)_{1-x}(\text{ZnO})_x$  thin films were prepared by spraying aqueous solution of tin oxide. This solution was prepared by dissolving 2.6653g of  $\text{ZnO}(\text{CH}_3\text{COO})_2 \cdot 2\text{H}_2\text{O}$  [which is a powder of white color, its molecular weight (266.53 g/mol.)] in 50 ml distilled water and 1.1285g of  $\text{SnCl}_2 \cdot 2\text{H}_2\text{O}$  [which is a powder of white color its molecular weight (225.63 g/mol.)] in 50 ml distilled water too. The dissolving weight ( $W_t$ ) of the materials  $\text{ZnO}(\text{CH}_3\text{COO})_2 \cdot 2\text{H}_2\text{O}$  and  $\text{SnCl}_2 \cdot 2\text{H}_2\text{O}$  respectively were determined by using the following equation [R. Kumaravelet *et al.*, 2007].

$$M = (W_t / M_{wt}) \times (1000 / V) \dots \dots \dots (1)$$

Where M: is the molar concentration, equal {0.2 for  $[\text{ZnO}(\text{CH}_3\text{COO})_2 \cdot 2\text{H}_2\text{O}]$  and 0.1 for  $[\text{SnCl}_2 \cdot 2\text{H}_2\text{O}]$ },  $M_{wt}$ : molecular weight, V: volume of distilled water. The weights of  $\text{ZnO}(\text{CH}_3\text{COO})_2 \cdot 2\text{H}_2\text{O}$  and  $\text{SnCl}_2 \cdot 2\text{H}_2\text{O}$  were measured by using electrical balance sensitive (KERN ABS120-4) four digits ( $10^{-4}$  g). Mixing the solutions with different  $W_t$ . 1% of x and leaving the solution for 24 hours to make sure that no residues were left and to ensure the homogeneity of the resultant solution. The resultant solution was sprayed on preheated glass substrates and silicon wafer to prepare  $(\text{SnO}_2)_{1-x}(\text{ZnO})_x$  thin films. When the solution is sprayed, the reaction takes place at the surface of the heated substrate. The resulting films were stable, whitish downhill to yellow in color, transparent, free from pinhole and have good adhesive properties.

### 2.2 The Parameters to Preparation Films

A simple homemade spray pyrolysis experimental setup was employed to prepare  $(\text{SnO}_2)_{1-x}(\text{ZnO})_x$  mixed thin films on glass substrates ( $35 \times 25 \times 1.35 \text{ mm}^3$ ) at a substrate temperature of  $400^\circ\text{C}$ . The difference in ZnO Vol.%(x) was achieved by mixing the aqueous solutions of 0.1 M of tin and zinc acetates to pre-determined volume ratio. The value of (x) in the solution was varied from 0.00 to 1.00 (x=0, 0.2, 0.4, 0.6, 0.8, 1). The mixed solutions which were then diluted with water formed the final spray solution and a total volume of 25 ml was used in each deposition. The

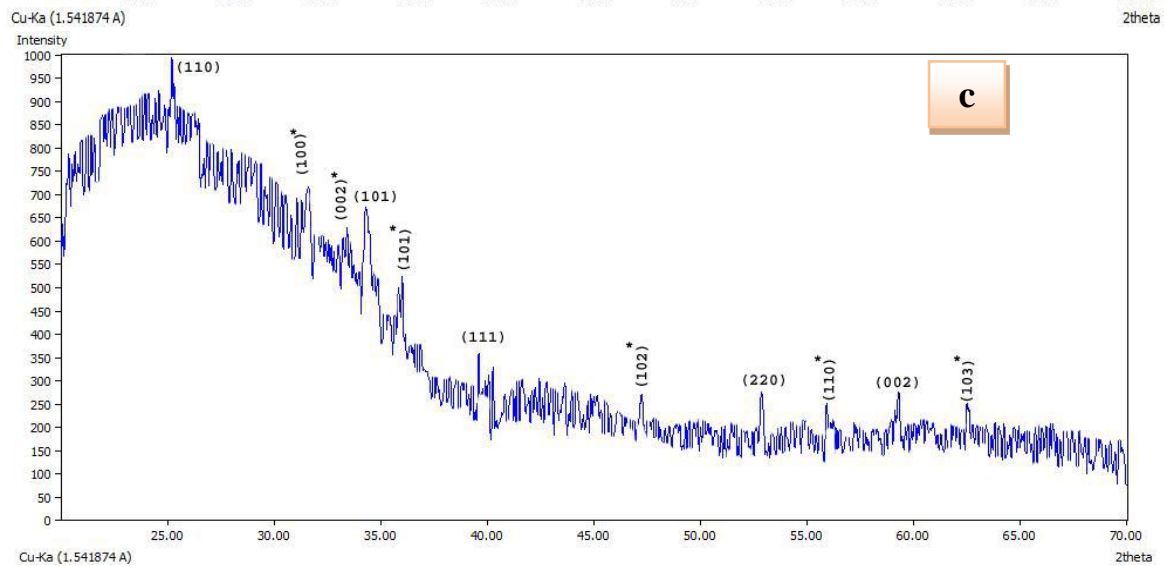
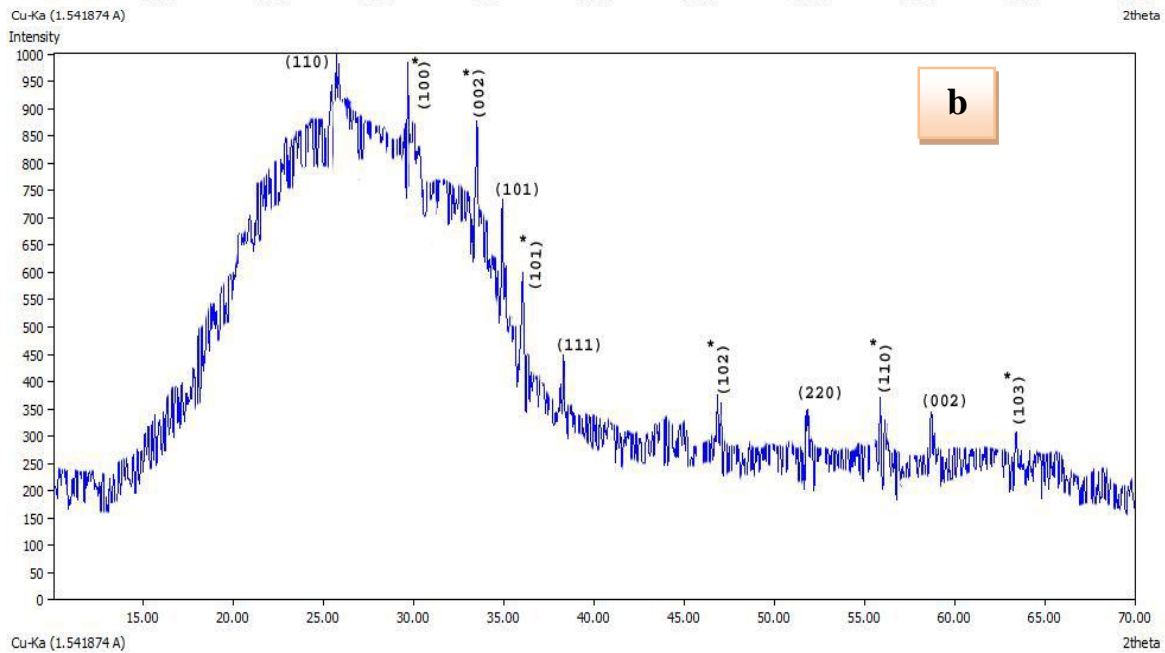
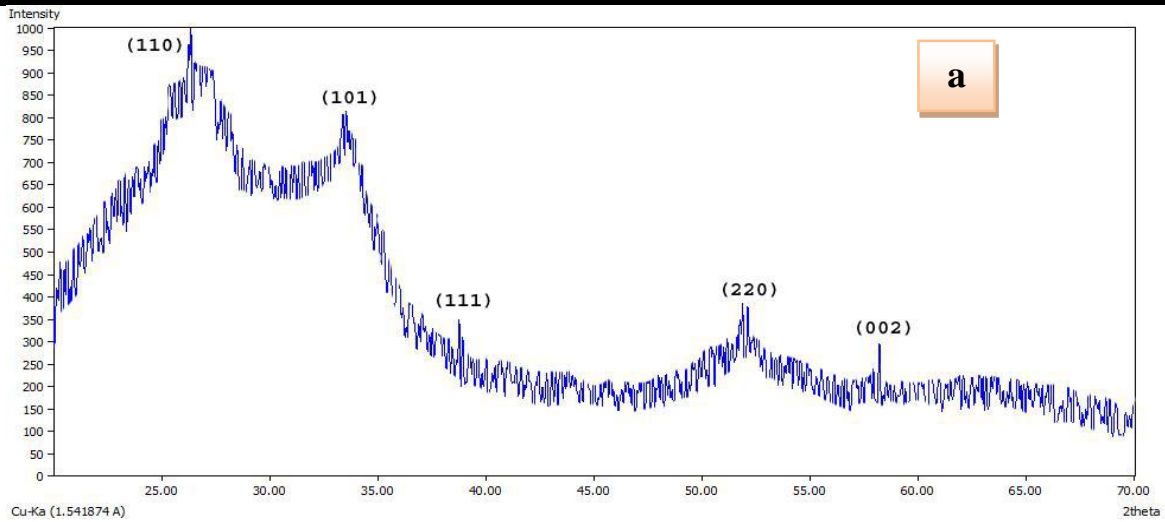
deposition parameters such as spray nozzle-substrate distance (30 cm), spray time (4s) and the spray interval (1 min) were kept constant. The carrier gas (filtered compressed air) flow rate was maintained at 6 l/min at a pressure of  $6.5 \times 10^4 \text{ Nm}^{-2}$ . X-ray diffraction (XRD) analysis was used to recognize the crystal structure of  $(\text{SnO}_2)_{1-x}(\text{ZnO})_x$  thin films. AFM study the surfaces of film materials deposited important to recognize how the distribution and arrangement of atoms on surfaces, and get to know the differences or homogeneity properties or attributes relating to each atom.

### III. RESULTS AND DISCUSSION

#### 3.1 X-Ray Diffraction Analysis (XRD)

XRD technique is used to find out the nature of the crystal structure and main crystalline phases and the direction of the films prepared in certain conditions, as well as to identify some of the structural parameters such as crystalline size and full width at half maximum (FWHM). The X-ray Diffraction investigation has been carried out for the prepared mixed thin films of  $(\text{SnO}_2)_{1-x}(\text{ZnO})_x$  in Fig.(1), for range from  $20^\circ$ - $70^\circ$  in  $2\theta$ . According to (PDF Entry No.: 00-005-0664 and No.:00-021-1250), International Centre for Diffraction Data (ICDD) cards, the structure of these films showed a polycrystalline. The interplaner spacing ( $d_{hkl}$ ) was determined using the Bragg relationship. From Fig.(1.a) when  $x = 0$  ( $\text{SnO}_2$  pure) sample, five peaks appears which could be related to (110), (101), (111), (220), and (002) planes of the tetragonal  $\text{SnO}_2$  phase were observed with cell parameters  $a = 4.7380 \text{ \AA}$  and  $c = 3.1880 \text{ \AA}$  at  $2\theta = (26.25^\circ, 33.26^\circ, 38.69^\circ, 52.95^\circ, 58.04^\circ)$  respectively. We observed that the peaks are the highest values (110) and (101) added to the presence of other peaks of the material is (111), (220), and (002) at  $2\theta = (26.25^\circ, 33.26^\circ, 38.69^\circ, 52.95^\circ, 58.4^\circ)$  where we note in this figure the value of ( $\beta$ ) (110) is characterized by the largest value with a significant difference from the other values. Were (110) is the preferred orientation of growth. In the Fig.(1.b), we note that the film contains the peaks of the materials  $\text{SnO}_2$  and ZnO where the peaks of the  $\text{SnO}_2$  (110), (101), (002), (220), and (111) at  $2\theta = (25.66^\circ, 35^\circ, 39.73^\circ, 51.84^\circ, 58.94^\circ)$  and ZnO peaks (100)\*, (002)\*, (101)\*, (102)\*, (110)\* and (103)\* at  $2\theta = (29.73^\circ, 33.68^\circ, 36.05^\circ, 46.57^\circ, 55.93^\circ, 63.68^\circ)$  where there are two peaks are (110), (100)\* where the first peaks of the angle was obtained by the angle of ( $25.66^\circ$ ). In Figure (1.c) we notice that the film has a high peak in addition to two peaks, where we notice there is a shifting from  $2\theta = (25.25^\circ)$  to  $2\theta = (25^\circ)$  for peak (110) and a shifting from  $2\theta = (33.68^\circ)$  to  $2\theta = (30.43^\circ)$  for the peak (002)\* and a shifting from  $2\theta = (33.91^\circ)$  the peak (101). In Figs.(1.d) and (1.e) we

observe that the preferred peak in the films is a shifting from  $2\theta = (25^\circ)$  to  $24.13^\circ$  and from  $2\theta = (25^\circ)$  to  $25.43^\circ$  respectively for the peak (110). From Fig.(1.f) when  $x = 1$  film ( $\text{ZnO}_{\text{pure}}$ ), the six diffraction peaks observed were identified as the reflections from (100)\*, (002)\*, (101)\*, (102)\*, (110)\* and (103)\* planes of hexagonal ZnO phase with a lattice parameters of  $a = 3.2490 \text{ \AA}$  and  $c = 5.2050 \text{ \AA}$ . The most prominent peak for the  $x = 1$  was the reflection from the (002)\* plane. The diffraction peaks corresponding to (100)\*, (002)\* and (101)\* planes were sharp in comparison to those from (102)\*, (110)\* and (103)\* planes. It is shown that the highest intensity is located at the directionality (002)\* with a direction perpendicular to the base. This tendency in crystallization is attributed to the Drift model, which is called the Survival of the Fittest model. We assume that the process of nucleation takes more than one direction in the early stages of films growth; these trends begin to compete as they grow. The nuclei continue to grow faster, while the growth of the other nuclei stops. This explains the growth of ZnO films toward (002)\* decomposition or sedimentation direction. It was observed that the granular size of the ZnO films was smaller than the granular size of the  $\text{SnO}_2$  films, indicating that the ZnO membrane in the selected conditions was better crystallized. The intensity of (110) remained conservative despite its added value and (101) reflections increasing with increase (ZnO) vol.%(until  $x = 0.6$ ) and then decreases slightly (at  $x = 0.8, 1$ ), while the intensity of (002)\* and (100)\* reflection increases with increasing (ZnO) vol.%( at  $x = 0.2, 0.4, 0.6$  and  $0.8$ ), also we note that the intensity of (110) reflection (at  $x = 0.2$ ) be the prominent and controlling for other peak in ( $\text{SnO}_2$ ) and (ZnO) thin film, this refers to the clear improvement in the crystalline properties of the film, where it is clear that (100)\* is the highest peak in intensity but (002)\* is the highest peak in intensity of (ZnO) films. For all films, the grain size (G.S) was calculated from the full width at half maximum (FWHM) ( $\beta$ ) of the preferred orientation diffraction peak by using the Debye-Scherrer's equation. Larger G.S and smaller  $\beta$  values indicate better crystallization of the materials. According to Table (1), we notice the (G.S) of (110) plane increase from (2.681, 7.738, 17.818 and 24.966) nm with increasing from Zn vol %  $x = (0, 0.2, 0.4, 0.6$  and  $0.8)$  respectively. Whereas the (G.S) of (002)\* plane decreases from (35.033, 9.464, 9.44 and 9.531) nm with increasing ZnO vol.%  $x = (0.2, 0.4, 0.6,$  and  $0.8)$  respectively. We also note the increase in the average of grain size with increasing ZnO Vol.%( $x = 0.2, 0.4$  and  $0.6$ ) this shows an improvement in the structural properties of the prepared films.



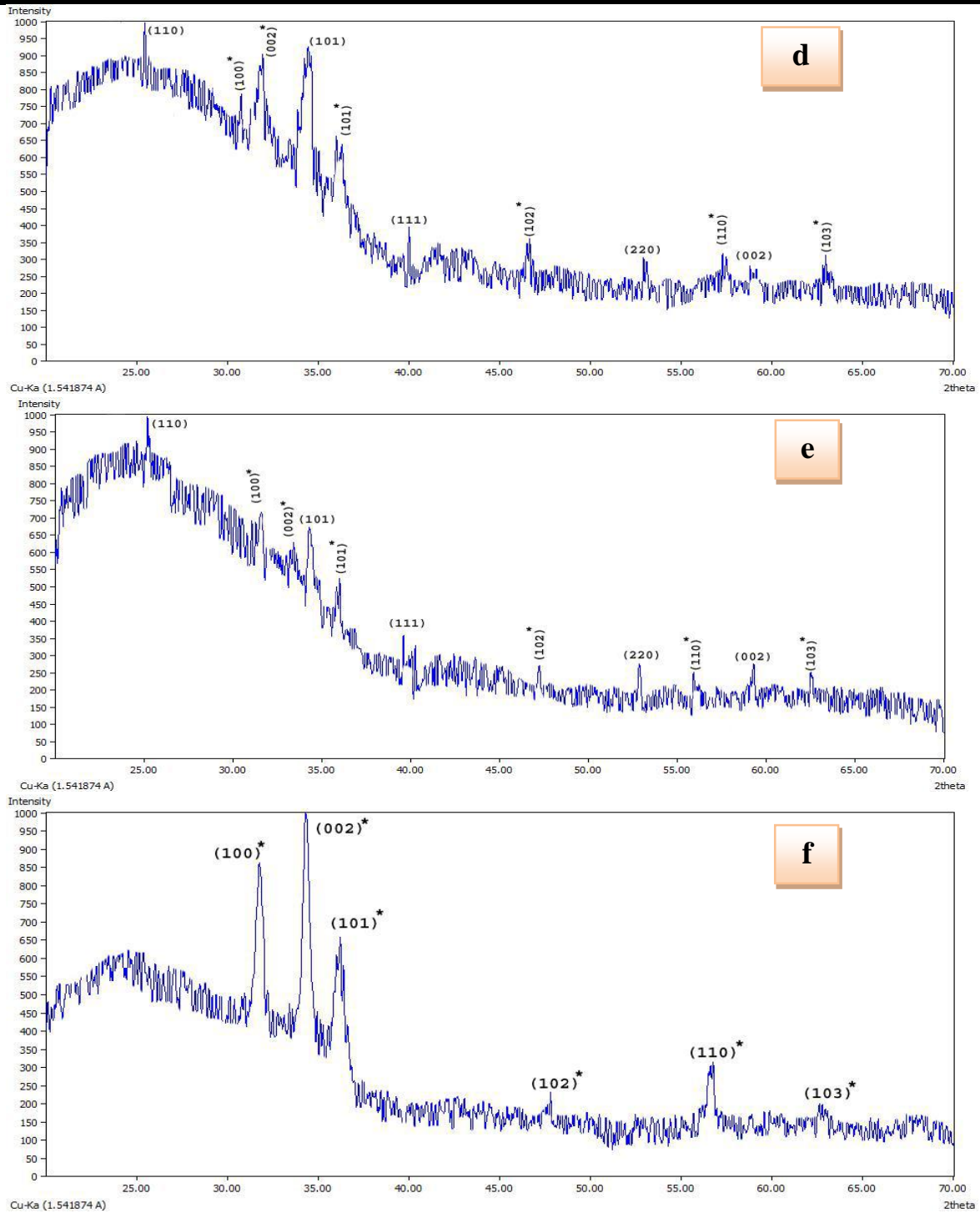


Fig.1: The X-ray diffraction patterns of the prepared films: (a)  $\text{SnO}_2$  pure , (b)  $(\text{SnO}_2)_{0.8}\text{ZnO}_{0.2}$ , (c)  $(\text{SnO}_2)_{0.6}\text{ZnO}_{0.4}$ , (d)  $(\text{SnO}_2)_{0.4}\text{ZnO}_{0.6}$ , (e)  $(\text{SnO}_2)_{0.2}\text{ZnO}_{0.8}$  and (f)  $\text{ZnO}_{\text{pure}}$ .

Table.1: X-ray diffraction parameters for  $(SnO_2)_{1-x}(ZnO)_x$  for different Vol.% of (x)

Sample	(hkl)	2θ (deg)	θ (deg)	d (nm)	FWHM(deg)	G.S (nm)	Average G.S (nm)
SnO <sub>2</sub>	(110)	26.25	13.26	0.336	3.043	2.681	21.277
	(101)	33.26	16.63	0.269	1.304	6.355	
	(111)	38.69	19.34	0.232	0.217	38.785	
	(220)	52.95	26.47	0.173	0.869	10.208	
	(002)	58.04	29.02	0.159	0.130	69.636	
SnO <sub>20.8</sub> ZnO <sub>0.2</sub>	(110)	25.66	12.83	0.3473	1.052	7.737	41.359
	(100)*	29.73	14.86	0.3006	0.526	15.620	
	(002)*	33.68	16.84	0.2662	0.236	35.032	
	(101)	35	17.5	0.2565	0.263	31.660	
	(101)*	36.05	18.02	0.2492	0.394	21.195	
	(111)	39.73	19.86	0.2270	0.210	40.108	
	(102)*	46.57	23.28	0.1951	0.5	17.290	
	(220)	51.84	25.92	0.1764	0.394	22.368	
	(110)*	55.93	27.96	0.1644	0.789	11.388	
	(002)	58.94	29.47	0.1567	0.447	20.387	
SnO <sub>20.6</sub> ZnO <sub>0.4</sub>	(110)	25	12.5	0.3563	0.456	17.818	31.460
	(100)*	30	15	0.2980	0.217	37.819	
	(002)*	30.43	15.21	0.2939	0.869	9.4643	
	(101)	33.91	16.95	0.2645	0.978	8.4866	
	(101)*	36	18	0.2496	0.652	12.803	
	(111)	40	20	0.2255	0.173	48.593	
	(102)*	46.73	23.36	0.1945	0.760	11.370	
	(220)	53.91	26.95	0.1701	0.543	16.391	
	(110)*	57.17	28.58	0.1612	1.086	8.319	
	(002)	59.13	29.56	0.1563	1.304	6.999	
SnO <sub>20.4</sub> ZnO <sub>0.6</sub>	(110)	24.13	12.06	0.3690	0.347	23.347	43.44
	(100)*	30.65	15.32	0.2918	0.217	37.877	
	(002)*	31.73	15.86	0.2821	0.869	9.494	
	(101)	34.34	17.17	0.2613	0.978	8.496	
	(101)*	35	17.5	0.2565	0.326	25.535	
	(111)	41.08	20.54	0.2198	0.652	13.003	
	(102)*	45.65	22.82	0.1988	0.369	23.312	
	(220)	52.6	26.3	0.1740	0.217	40.745	
	(110)*	55.65	27.82	0.1652	0.173	51.629	
	(002)	58.26	29.13	0.1584	0.760	11.948	
SnO <sub>20.2</sub> ZnO <sub>0.8</sub>	(110)	25.43	12.71	0.3504	0.326	24.966	29.70
	(100)*	31.3	15.65	0.2859	0.652	12.645	
	(002)*	33.26	16.63	0.2695	0.869	9.531	
	(101)	34.56	17.28	0.2596	0.760	10.930	
	(101)*	35.86	17.93	0.2505	0.782	10.665	
	(111)	39.56	19.78	0.2279	0.978	8.532	
	(102)*	47.17	23.58	0.1927	0.347	24.262	
	(220)	52.82	26.41	0.1734	0.543	15.943	
	(110)*	56.08	28.04	0.1640	0.847	10.457	
	(002)	59.34	29.67	0.1558	1.086	8.277	
ZnO pure	(103)*	62.6	31.3	0.1484	0.217	42.038	15.80
	(100)*	31.58	15.79	0.2834	0.5	16.506	
	(002)*	34.57	17.28	0.2596	0.46	18.081	
	(101)*	36.3	18.15	0.2476	0.652	12.818	
	(102)*	47.72	23.86	0.1906	0.543	15.991	
	(110)*	56.74	28.37	0.1623	0.435	20.746	

**3. 2Atomic Force Microscope (AFM)**

The study of film surfaces is deposited important to recognize how the distribution and arrangement of atoms on surfaces, and get to know the differences or homogeneity properties or attributes relating to each atom separately, can through microscopic analysis AFM study the effect of the parameters (thickness, temperature, method of preparation etc.) on the properties of film material deposited. As well as analysis of the AFM can calculate the thickness of film, roughness and grain size, and gives an illustrative picture of the distribution of the particle size of the crystal on the surface rate. Figs.(2) to (3) show the AFM images were measured over an area of (2000nm × 2000nm). The average grain size of the particles is in nanoscale. Root mean square, roughness, total grain size values were listed in Table (2). Fig.(2a, b, c, d,e and f) shows the three-dimensional images of the (SnO<sub>2</sub>)<sub>1-x</sub>(ZnO)<sub>x</sub> thin films it's found that surface thickness rats this value represents the thickness of the film surface roughness, which account for the highest crystalline granular tops on the surface.

Fig.(3a, b, c, d,e and f) shows the graph on the distribution of growth granular aggregates on the surface of the deposited films. The growth of small grains with increasing ZnO Vol.% leads to a decrease in the surface roughness. Table (2) shows the grain size of (SnO<sub>2</sub>)<sub>1-x</sub>(ZnO)<sub>x</sub>,we can observe that grain size increases with increasing of the mixing ratios, this result agree with XRD results. Also, the table(2) shows the roughness for (SnO<sub>2</sub>)<sub>1-x</sub>(ZnO)<sub>x</sub> films and the root mean square (RMS), where results increases in roughness rate and the root mean square (RMS) with increasing the mixing ratios it is obvious that surface is rough, the increase of root mean square leads to increase in crystalline growth in vertical direction[Hoon, JW. *et al*, 2011].

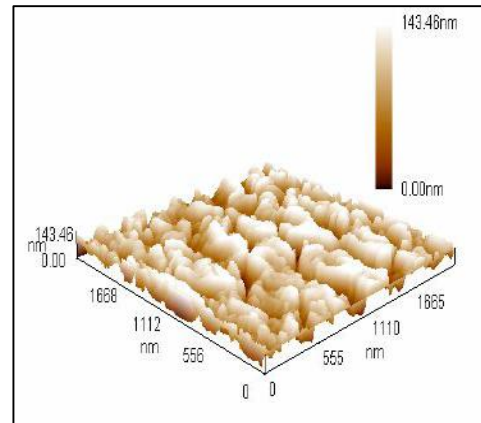
Table.2: AFM data for (SnO<sub>2</sub>)<sub>1-x</sub>(ZnO)<sub>x</sub> thin films at different Vol.% of (x).

Sample	Roughness (nm)	RMS (nm)	Average Diameter (nm)
SnO <sub>2</sub> pure	33.6	39.3	58.57
(SnO <sub>2</sub> ) <sub>0.8</sub> ZnO <sub>0.2</sub>	45	52.9	78.12
(SnO <sub>2</sub> ) <sub>0.6</sub> ZnO <sub>0.4</sub>	50	57.7	91.08
(SnO <sub>2</sub> ) <sub>0.4</sub> ZnO <sub>0.6</sub>	51.5	59.2	98.47
(SnO <sub>2</sub> ) <sub>0.2</sub> ZnO <sub>0.8</sub>	51.6	59.8	102.71
ZnO pure	54	61.1	108.72

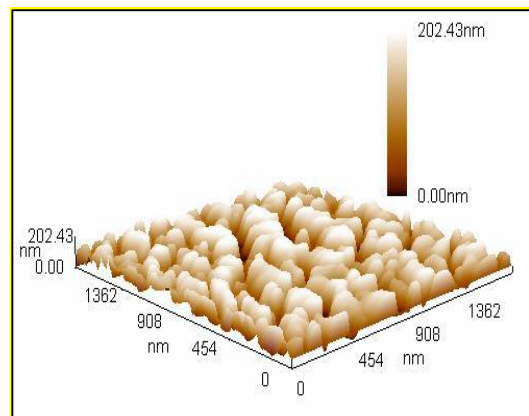
**IV. CONCLUSION**

The XRD studies confirmed the tetragonal SnO<sub>2</sub> phase and hexagonal ZnO phase. Further, it is understood that the crystallinity of SnO<sub>2</sub> increases with increasing ZnO vol.%. The calculated mean crystallite size of the selected planes of SnO<sub>2</sub> and ZnO were found varying between (21.27

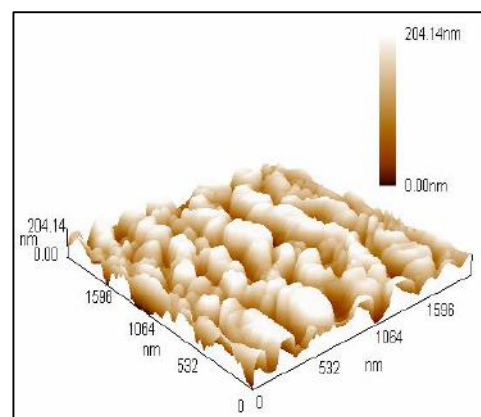
and 15.80) nm. The variation of crystallite size corroborates with XRD patterns and the growth of small grains with increasing ZnO Vol.% leads to a decrease in the surface roughness. We can observe that grain size increases with increasing of the mixing ratios, this result agree with XRD results. we can observe the roughness for (SnO<sub>2</sub>)<sub>1-x</sub>(ZnO)<sub>x</sub> films and the root mean square (RMS), where results increases in roughness rate and the root mean square (RMS) with increasing the mixing ratios it is obvious that surface is rough, the increase of root mean square leads to increase in crystalline growth in vertical direction.



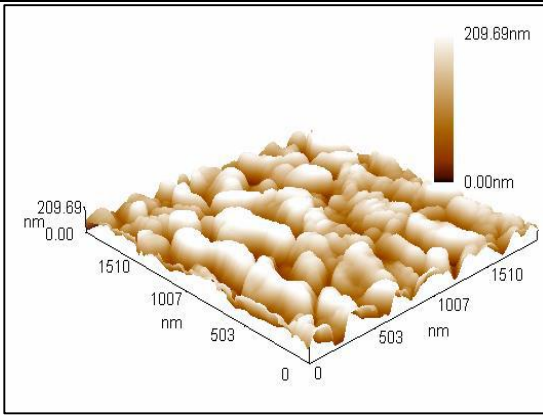
(a)



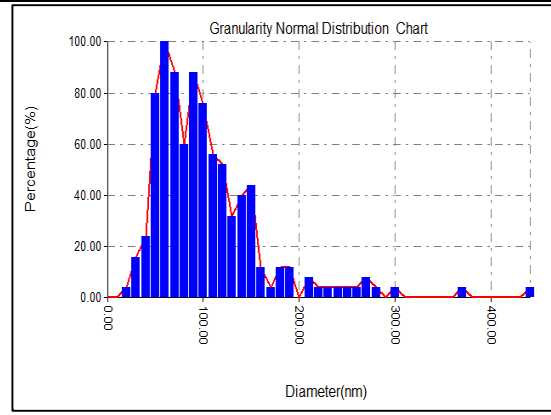
(b)



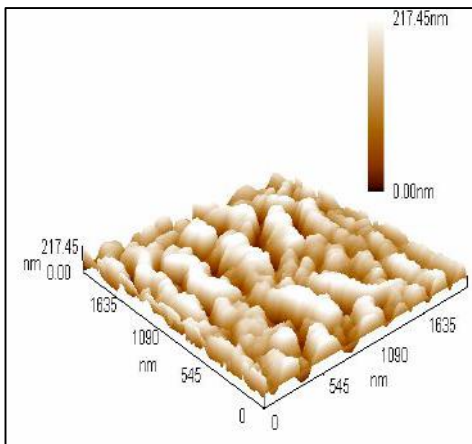
(c)



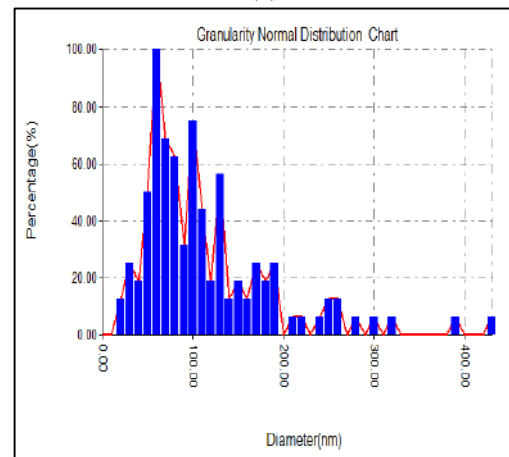
(d)



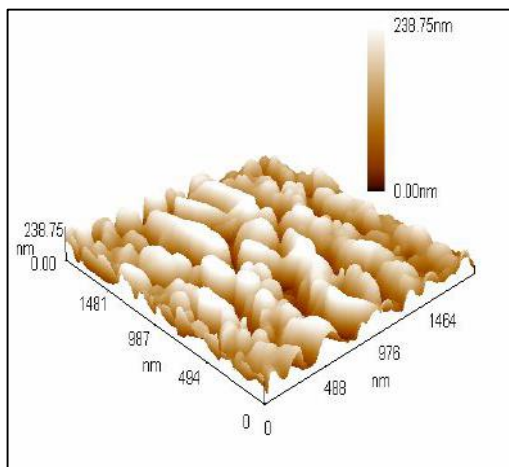
(a)



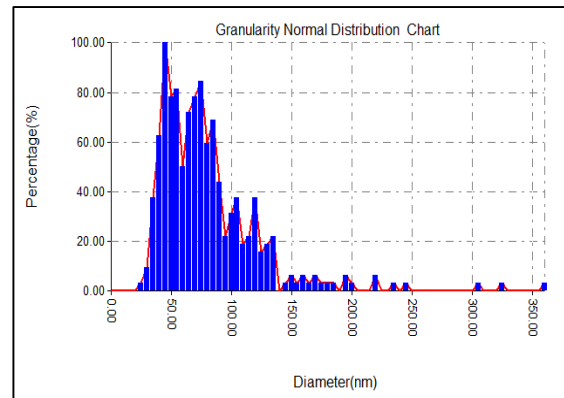
(e)



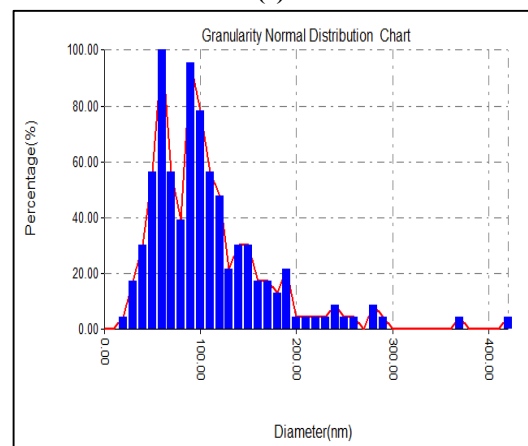
(b)



(f)

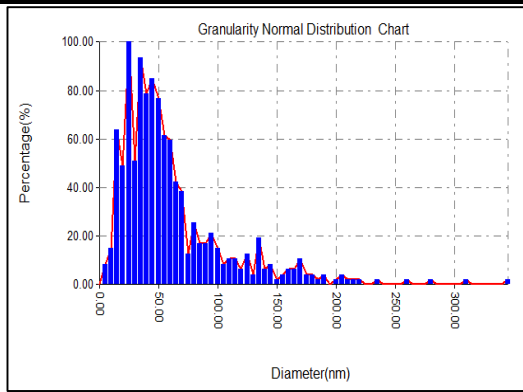


(c)

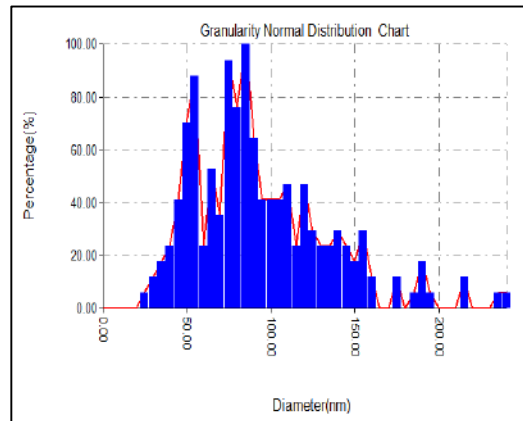


(d)

Fig.2: 3-D images of the prepared thin films: (a)  $\text{SnO}_2$  pure, (b)  $(\text{SnO}_2)_{0.8}\text{ZnO}_{0.2}$ , (c)  $(\text{SnO}_2)_{0.6}\text{ZnO}_{0.4}$ , (d)  $(\text{SnO}_2)_{0.4}\text{ZnO}_{0.6}$ , (e)  $(\text{SnO}_2)_{0.2}\text{ZnO}_{0.8}$  and (f)  $\text{ZnO}$  pure.



(e)



(f)

Fig.3: Granularity distribution for the prepared thin films: (a)  $\text{SnO}_2$  pure, (b)  $(\text{SnO}_2)_{0.8}\text{ZnO}_{0.2}$ , (c)  $(\text{SnO}_2)_{0.6}\text{ZnO}_{0.4}$ , (d)  $(\text{SnO}_2)_{0.4}\text{ZnO}_{0.6}$ , (e)  $(\text{SnO}_2)_{0.2}\text{ZnO}_{0.8}$  and (f)  $\text{ZnO}$  pure.

### REFERENCES

- [1] Baleva, M.I.; Bozukov L.N. and Tuncheva, V.D., J. Phys. Chem., Vol. 98, p.13308,(1994).
- [2] Cruz, J.; Delgado, G.; Perez, R. ; Sandoval, S.; Sandoval, O. Romero, C.I. Marin J. and Angel, O., Thin Solid Films, Vol.493,p.83, (2005).
- [3] Elangovan E. and Ramamurthi, K., Appl. Surf. Sci. Vol.249,p. 183,(2005).
- [4] Ferrer, I.J., Electrochim. Acta, Vol.38, p.2199,(1993).
- [5] Ferro, R.; Rodriguez, J.A. Vijil, O. Acevedo A. and Puente, G., Phys. Status Solidi, A Appl. Res., Vol.177,p.477,(2000).
- [6] Galicia, D.M.; Perez, R.; Sandoval, O.; Dandoval, S.; Delgado, G.; Romero, C.I., Thin Solid Films, Vol.31,p. 105,(2000).
- [7] Hoon, JW.; Chan, KY.; Krishnasamy, J.; Tou, TY.; Knipp, D., Appl. Surf. Sci., 257, 2508,( 2011).
- [8] Hosono, H.; Yamashita, Y.; Ueda N. and Kawazoe, H., Appl. Phys. Lett., Vol.68, p.661,(1996).
- [9] Ilcan, S.; Caglar, Y. Caglar, M. and Yakuphanoglu, F., "Structural, Optical and Electrical Properties of F-doped ZnO Nanorod Semiconductor Thin Films Deposited by Sol-Gel Process", Applied Surface Science, Vol. 255, pp. 2353-2359, (2008).
- [10] Kirkbir, F.; Katz, D.; Lysse R. and Mackenzie, J.D., J. Mater. Sci., Vol.27,p.1748,(1992).
- [11] Koh, S. ; Han, Y.; Lee, J.; Yeo, U. ; Cho, J., Thin Solid Films ,Vol.496,p.81,(2006).
- [12] Kumaravel, R.; Krishnakumar, V.; Ramamurthi, K.; Elangovan E. and Thirumavalavan, M., " Deposition of  $(\text{CdO})_{1-x}(\text{PbO})_x$  Thin Films by Spray Pyrolysis Technique and Their Characterization", Journal of Thin Solid Films, Vol.515, pp.4061–4065, (2007).
- [13] Martins, R.; Fortunato, E. Nunes, P. Ferreira, I. Marques, A. Bender, M. Katsarakis N. and Cimalla, V.; G. Kiriakidis, J. Appl. Phys., Vol. 96,p.1398, (2004).
- [14] Ocampo, M.; Sabastian P.J. and Campos, J., Phys. Status Solidi, A Appl. Res., Vol.143, p.29,(1994).
- [15] Ramakrishna Reddy, K.T.; Sravani C. and Miles, R.W., J. Cryst. Growth, Vol.184/ 185,p.1031,(1998).
- [16] Sarma H. and A. Srinivasan, J. Mater. Sci. Vol.39,p.7085, (2004).
- [17] Sivakumar, R. P. Manisankar, M. Jayachandran and C. Sanjeeviraja, Sol. Energy Mater. Sol. Cells, Vol.90,p.2438, (2006).
- [18] Subramanyam, T.K.; G. Mohan Rao and S. Uthanna, Mater. Chem. Phys., Vol.69, p.133, (2001).
- [19] Sze, S. M., "Physics of Semiconductor Devices", John Wiley and Sons, (1981).
- [20] Thangaraju B. and P. Kaliannan, " Optical and structural studies on spray deposited  $\alpha$ -PbO thin films", Semicond. Sci. Technol., Vol. 15, p.542, (2000).
- [21] Trinquier G. and Hoffman, R., J. Phys. Chem., Vol.88,p.6696, (1984).
- [22] Verky A.J. and Fort, A.F., "Transparent conducting cadmium oxide thin films prepared by a solution growth technique", Thin Solid Films ,Vol. 239,p. 477, (1994).